Composite Materials
2021; 5(1): 17-29
http://www.sciencepublishinggroup.com/j/cm
doi: 10.11648/j.cm.20210501.12

Review Article

Layered 2D Transition Metal Dichalcogenides (MX_2; M=Mo, W; X=S, Se, Te) Nanosheets and Their Composites for Photocatalytic Applications: A Review

Divya[1], Shivam Rai[2], Tina Chakrabarty[3], Arnab Kanti Giri[4, *]

[1]Department of Chemistry, Aligarh Muslim University, Aligarh, India

[2]Department of Applied Chemistry, Gautam Buddha University, Greater Noida, India

[3]Research and Development, Tata Steel Ltd., Jamshedpur, India

[4]Department of Chemistry, Karim City College, Jamshedpur, India

Email address:

giri.arnabkanti54@gmail.com (A. K. Giri)

[*]Corresponding author

To cite this article:

Divya, Shivam Rai, Tina Chakrabarty, Arnab Kanti Giri. Layered 2D Transition Metal Dichalcogenides (MX_2; M=Mo, W; X=S, Se, Te) Nanosheets and Their Composites for Photocatalytic Applications: A Review. *Composite Materials*. Vol. 5, No. 1, 2021, pp. 17-29.
doi: 10.11648/j.cm.20210501.12

Received: June 17, 2021; **Accepted**: July 2, 2021; **Published**: July 13, 2021

Abstract: Current, in-depth research on layered two-dimensional transition metal dichalcogenides (2D-TMDCs) has been triggered by a progression of investigative theoretical predictions and experimental observations of unanticipated electronic, optical and photochemical properties in nanosheets and their composites of this family of materials, especially their most archetypal member, MoS_2. MoS_2 nanosheets show a fantastic array of properties to be a potential candidate as an active photochemical agent, thus contributing to the gateway of an immense number of problems. However, from the past 2-3 years, the other family members, MoX_2 (X=Se, Te) and WX_2 (X=S, Se, and Te), are stepping out of the shadows of the famous molybdenum disulfide and establishing their own identity. This review aims to arrange and combine information on photocatalytic hydrogen production, water splitting, dye degradation, visible light photocatalytic activity, photocatalytic CO_2 reduction, and environmental remediation of layered 2D-TMDCs nanosheets and their composites. Due to the popularity of MoS_2, the central focus of the review is on $MoSe_2$, $MoTe_2$, WS_2, WSe_2. This work presents a systematic report on the applications of various 2D metal dichalcogenides as a whole, exploring their prime role in enhancing individual performance like the evolution of hydrogen gas, reduction of CO_2, and degradation of toxic dyes or pollutants. All such treatments are of utmost significance for having a better environment to live. Thus, this specifies the importance of 2D-TMDCs towards the attainment of a sustainable homeland. In recent years WTe_2 has emerged as a potential candidate for giant magnetoresistance and superconductivity. However, in the case of photocatalytic applications, it is not very economical for commercial development. Therefore, WTe_2 is excluded from our discussion.

Keywords: Transition Metal Dichalcogenides Nanosheets, HER, Dye Degradation, CO_2 Reduction, Water Splitting, Visible-Light-Driven Photocatalysis

1. Introduction and Background

The successful examination of graphene over the past decade has given rise to extensive research devotion towards the graphene-like 2D layered materials, and the house of 2D layered transition metal dichalcogenides (TMDCs) has acquired significant attention over the past few years as an emerging novel class of nanomaterials for foundational studies and demanding applications owing to their fascinating properties [1-3]. A class of materials that has become a thriving research field ranging from photocatalysis [4] to water splitting [5], solar cells [6], lithium-ion batteries [7], Opto-electronics [8], sensors [9]. In recent years, 2D-layered TMDCs: MoS_2, $MoSe_2$, $MoTe_2$, WS_2, WSe_2 have become a

research hotspot due to their promising photocatalytic applications such as photocatalytic hydrogen production, dye degradation, water splitting, visible light photocatalysis, photocatalytic CO_2 reduction, and environmental remediation [10-14]. Due to its vast history and ideal 2D structure, MoS_2 is the flagship of 2D TMDCs [15]. From the perspective of a photocatalyst, MoS_2 (single- or few-layer) nanosheets possess exceptional photo-induced catalytic ability because of suitable bandgap (i.e., ca. 1.8 eV single-layer MoS_2). The high charge-carrier mobility and the large surface-to-volume ratio of MoS_2 nanosheets show remarkable advantages for photo-electrocatalysis. Most of the methods used for the isolation/preparation of graphene are also plausible for MoS_2 nanosheets due to the layered structure similar to graphene. Photocatalytic hydrogen evolution, from the perspective of hydrogen evolution reaction, has always been the center of attention for research. Noble metals, such as Platinum, Gold, and Palladium, were traditionally involved as catalysts for photocatalytic hydrogen production but are expensive and scarce. Therefore, MoS_2 and $MoSe_2$ are the most promising candidates to replace them because of their superior catalytic ability in photocatalytic hydrogen production [16-18]. Due to its outstanding application potential in various fields and its excellent physical and chemical properties, $MoSe_2$ has gradually become the main research topic in photocatalysis. It has properties such as the back-gate effect and solid lubrication, which other transition metal disulfide lack. By applying any external mechanical strain or electric field, the bandgap of $MoSe_2$ can be tuned effectively. Following the popularity of MoS_2 and $MoSe_2$, the attention is shifting towards WS_2, WSe_2, WTe_2 [19-22]. In general, WX_2 shows characteristics that demand a wide range of applications. WS_2 has shown similar characteristics to that of MoS_2 as a co-catalyst and Cadmium Sulfide for the photocatalytic water splitting for hydrogen production since the performance was similar to those of noble metals. For various photochemical and photoelectrochemical applications, the optoelectric properties of the van der Waals heterojunctions of MoS_2/WS_2 and MoS_2/WSe_2 have shown promising potentials. WSe_2 provides a firm and ample interlayer architecture suitable for solid-state diffusion of counter-ions. The effective factor for the considerable amount of specific capacity is facile diffusion. The advancements in this short period clearly show the bright horizon ahead for tungsten dichalcogenides [23-25]. Compared with the molybdenum counterparts, tungsten is more abundant in the earth's crust. Thus, cheaper and less toxic. Also, the large tungsten atoms can effectively tune the TMDCs properties by altering the 2D structure. In most of the applications, the general behavior of WX_2 (X=S, Se, Te) is similar to that of MoX_2 (X=S, Se, Te), but the real advantage of WX_2 is in the manipulation of the lattice, e.g., by strain engineering. The popularity of molybdenum dichalcogenides has somehow overshadowed the potentials of tungsten dichalcogenides. The industrial consumption of molybdenum is currently higher while having a lower number of mineral resources. Hence the commercial availability of tungsten becomes more favorable for future industrial applications. Therefore, the key differentiating aspect of this review article is that we have collected recent advances on photocatalytic applications of WS_2 and WSe_2 along with MX_2 (X=S, Se, Te) to provide a general overview to the reader and confidence to researchers for further exploring the territory of tungsten dichalcogenides. Also, we would like to draw the readers' attention towards this point that the intention of this review is not to serve as an exhaustive data-gathering and clumsy listing of references but rather to present an overview healthily on the layered 2D-TMDCs photocatalytic applications in an absolute yet concise way. Our review's main objective is to portray the current science of layered 2D-TMDCs nanosheets from a photocatalytic application-oriented perspective through a critical and comparative presentation approach. Throughout the text, special attention is directed towards consistent terminology, notation, and abbreviations in an effort and desire that this review article becomes a major reference work for photocatalytic applications of layered 2D-TMDCs nanosheets for many years. On the other hand, WTe_2, an important member of this group which in recent years has shown large magnetoresistance, i.e., change of electrical resistivity with an applied magnetic field, a rare and remarkable property of limited materials used for the development of magnetic sensors, magnetic memory, spintronics [28]. However, in the case of photocatalysis and other applications, WTe_2 is not very economical for commercial development as Te is too expansive regardless of the performance. Also, while comparing molybdenum and tungsten telluride, it is seen that though the electrocatalytic performance of bulk WTe_2 is way better than its $MoTe_2$ counterpart, exfoliation, playing a major role, reverses the supremacy [29-30]. Therefore, WTe_2 is not discussed in this paper.

Some insightful reviews discuss transition metal dichalcogenides nanomaterials-synthesis, properties, and applications, particularly on molybdenum and tungsten dichalcogenides. Chhowalla and colleagues' review provides a highly insightful and unique thorough discussion of the chemistry of transition metal dichalcogenides nanosheets in a rational way that presents important production methods and applications [31]. Another to the point review by Samadi and colleagues gives detailed and accurate information on science, production methods, and different applications such as (Opto) electronics, sensors, energy storage, and catalysis of all group 6 transition metal dichalcogenides nanomaterials in a cognitive framework [32]. Although the literature survey shows many review articles on different members of molybdenum dichalcogenides and tungsten dichalcogenides, devoted to specific applications but an overall treatment of photocatalytic applications, which is necessary, is still lacking. Therefore, this manuscript focuses on molybdenum dichalcogenides and attempts to highlight tungsten dichalcogenides' potential by collecting the noticeable findings reported in the literature during the past few years.

2. Photocatalytic Applications

2.1. Photocatalytic Water Splitting and HER

For hydrogen production, the water splitting in the presence of sunlight has attracted immense attention as a green route for converting solar energy into renewable and clean hydrogen energy. It also serves as a promising approach to solve environmental problems because of fossil fuels and meet the energy demands due to its ability to use the natural energy source [33-36]. Recently, two-dimensional (2D) transition metal dichalcogenides (TMDCs) semiconductors like MoS_2 [37], $MoSe_2$ [38], WS_2 [39], WSe_2 [40] have gained much curiosity due to their potential photocatalytic activity in visible region [41]. MoS_2 (Single- or few-layered) exhibits many superior characteristics compared to the bulk material because of its higher specific surface area and more exposed active sites, direct bandgap, which is better for hydrogen evolution reaction (HER) as a photocatalytic application [42-43]. Also, it is worth informing that the MoS_2 is mostly used as a co-catalyst for CdS-based or other photocatalysts in hydrogen evolution, as it can inhibit the recombination of photo-generated charge carriers [44-46]. The 2D-2D MoS_2/g-C_3N_4 photocatalyst contains 0.75% MoS_2, and the optimized 2D/1D TiO_2/MoS_2 heterojunction containing 60 wt.% MoS_2 showed the highest hydrogen evolution rate of 1155 μmol·h^{-1}·g^{-1}. Also, an evident quantum yield of 6.8% at 420 nm monochromatic light and 171.24 μmoL·g^{-1}·h^{-1}, respectively, is achieved simply because the charge separation and transfer get accelerated in the presence of two-dimensional nanointerfaces [47-48].

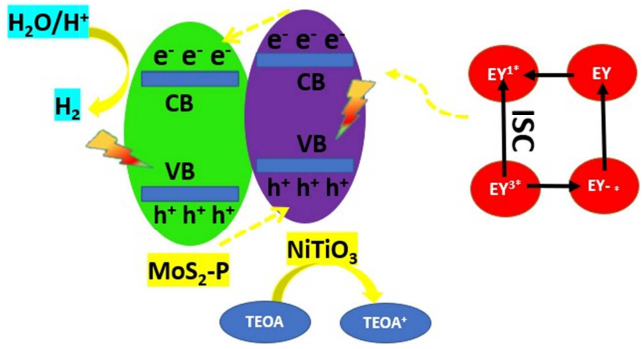

Figure 1. *Mechanism depicting the photocatalytic hydrogen evolution reaction.*

Metal selenides, as well as metal sulfides both, have metalloid properties, but the metalloid character of selenium is weaker than that of the sulfur, the ionic bond of metal selenide is weaker, and thus, this leads to the narrower bandgap and higher amount of absorption in visible light [49]. Also, because of the narrower bandgap, the carrier's mobility in metal selenide will always be considerably more than that of the metal sulfides, accounting for better performance. The band structure of $MoSe_2$ can be attuned with a bandgap value as high as 1.7-1.9 eV [50-52], which favors the comprehensive visible light response and successfully expands the light absorption region [53]. Simultaneously, during the HER process, the unsaturated Se atoms at the edge and the ones at defective points display magnificent catalytic activity [54]. Such characteristics of $MoSe_2$ proffer it as an exemplary catalyst for HER with high current density. Recent studies also show that $MoSe_2$ with sheet-like morphology being coupled with $ZnIn_2S_4$ [55] and g-C_3N_4 [56] and uniform hollow $MoSe_2$/CdS-CdSe [57] nanocomposite represents amplified photocatalytic hydrogen evolution activity. The main reason behind the higher photocatalytic activity is the broader access for the reach to the sunlight's spectrum, more number of active edge sites, higher charge transfer channels due to multicomponent presence heterojunction along with the high chemical and photostability. Molybdenum telluride nanowire has a bandgap of 1.60 eV, which depicts highly active material under visible light irradiation. It represents excellent HER performance along with optical properties [58]. The conduction band level in $MoTe_2$ is higher than the usually considered MoS_2, $MoSe_2$, and WS_2 [59] and thus is expected to show more amount of hydrogen evolution activity. Also, doping Cu cation has resulted in the improved HER activity of the $MoTe_2$ nanosheets and RGO/$MoTe_2$ nanosheet hybrids [60].

The 1T-WS_2/g-C_3N_4 composite with optimum 27% 1T-WS_2 exhibits a remarkably enhanced photocatalytic H_2 production rate of 1021 μmol h^{-1} g^{-1} and thus reflects an excellent photocatalytic H_2 production stability. Few reports on the loading WS_2 co-catalysts on the semiconductor for the enhanced photocatalytic H_2 production performances as loading lowers the activation barriers for oxygen and hydrogen and accounts for the effective charge separation at the same time [61-63]. The graphene-like WSe_2 is a suitable catalyst for high-yielding hydrogen evolution like $TeSiO_2$/WSe_2-graphene-TiO_2 photocatalyst due to the proper band alignment of the two heterostructures involved [21, 64]. The RGO/1TWSe_2: Sn nanosheet hybrids also reflect an enhanced activity and stability for hydrogen evolution as doping Sn cation and blending with RGO enhances the interface induced effect, which helps in catalyzing the hydrogen evolution reaction [65]. Table 1 represents the maximum hydrogen evolution rate for various combinations of metal dichalcogenides, from single layer to two-dimensional layer to different heterostructure, acting as a photocatalyst under specific light irradiation. It reflects that EY/1T-$MoSe_2$ and MoS_2 as a co-catalyst with CdS leads to higher hydrogen evolution. From the review, it can be concluded that among all the metal dichalcogenides considered, MoS_2, $MoSe_2$, $MoTe_2$, WS_2, and WSe_2, the maximum hydrogen evolution rate is observed with molybdenum telluride because of the higher conduction band level. As illustrated by Figure 1, when visible light is irradiated, there will be an electron from the valence band to the conduction band in MoS_2-P and $NiTiO_3$. Now because of the strong interaction among MoS_2-P and $NiTiO_3$ and the presence of the thermodynamic driving force, the photo-generated electrons that were transferred from the VB to CB will be transferred to the lower conduction band for the evolution of hydrogen gas, which is also responsible for the effective inhibition of the recombination of holes and electrons [66].

Table 1. *Photocatalytic hydrogen evolution data of MoS_2, $MoSe_2$, and WS_2 as reported in various literature reports.*

Serial Number	Photocatalyst	Irradiation	Hydrogen evolution rate (μmol. $g^{-1}h^{-1}$)	Reference
1.	Eosin Y (EY)/MoS_2/RGO	300 W Xenon lamp	2000	[67]
2.	EY/RGO/MoS_2	100 W Halogen lamp	3000	[68]
3.	EY/1T-$MoSe_2$	100 W Halogen lamp	75000	[69]
4.	CdS/Graphene/MoS_2	300 W Xenon lamp	9000	[70]
5.	CdS/WS_2	400 W Xenon lamp	4200	[71]
6.	TiO_2/1T-WS_2	300 W Xenon lamp	2570	[72]
7.	TiO_2/MoS_2/grapheme	350 W Xe lamp	2000	[73]
8.	p-MoS_2/n-rGO	300 W Xe lamp	24.8	[74]
9.	$MoSe_2$/g-C_3N_4	300 W Xe lamp	136.8	[75]
10.	TiO_2/$MoSe_2$	300 W Xe lamp	468.2	[52]
11.	TiO_2/$MoSe_2$/γ-graphene	300 W Xe lamp	800	[76]
12.	MoS_2 nanoflakes	300 W Xe lamp	122.5	[77]
13.	CdS/MoS_2@Ni_2P	solar simulator	7276	[78]
14.	MoS_2 quantum dots	450 W Xe lamp	24.3	[79]
15.	Few-layer MoS_2 nanosheets	300 W Xe lamp	1241.3	[80]

2.2. Photocatalytic Dye Degradation

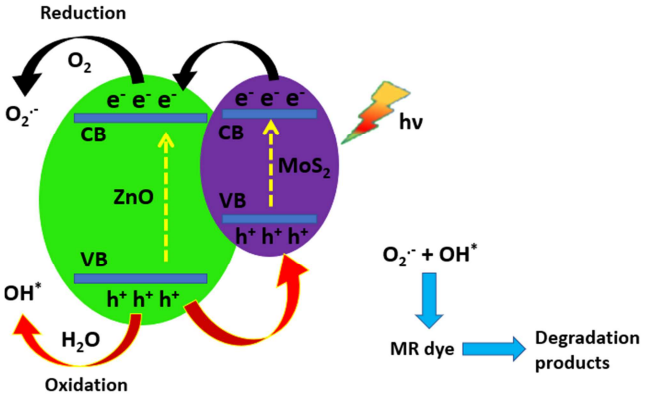

Figure 2. *Mechanism representing the degradation of methyl red dye over ZnO-MoS_2 composite.*

Photocatalysis is a promising method for wastewater treatment as it helps in the conversion of more toxic organic pollutants into less toxic products. Many dyes get accumulated in water bodies because of untreated loading, cationic like Rhodamine B (RhB), Methylene Blue (MB) or anionic like Congo Red (CR), Methyl Orange (MO), and their degradation is an essential factor because of their toxic effect where MoS_2 plays a unique role [81-83]. All the four TMDs were taken into account, and because of the presence of fully exposed active edges along with the lower rate of electron-hole recombination, WS_2 [84], MoS_2 [85], $MoSe_2$ [86-88], and WSe_2 [89], represents appreciable performance for the degradation of Rhodamine B dye in the presence of visible light irradiation. Under UV-Visible light, pristine MoS_2 displays photodegradation efficiencies between 30% to 46.9% for Methylene Red and 23.3% to 44% for Methylene Blue from 30 to 120 min time exposure, respectively. This enhanced performance's prime reason can be attributed to Au nanoparticles' availability, which acts as charge trapping sites in the nanostructures [90]. To be mentioned, the best photocatalytic activities are exhibited by the flower-like MoS_2, where its 2D stacked petals, having abundant active sites, significantly affect the photocatalytic efficiency [91]. Degradation of compounds NB, PNP, and 2, 4- DNP by $MoSe_2$ nanospheres follows the pseudo-first-order kinetics [92].

The overall mechanism for photocatalytic activity includes two significant steps;

(i) There should be superior photo-absorption in the region of interest.

(ii) The photo-induced electron-hole pairs, which are of prime importance, their generation, separation, and transfer should be efficient and smooth.

$MoSe_2$ is also helpful in the degradation of MB, MO [93-95], due to the accelerated detachment of photo-induced charge carriers and the more specific area, where the vertically oriented $MoSe_2$ nanosheets show an enhanced degradation on grapheme. $MoSe_2$-PPy nanocomposite is also a promising photocatalyst for the degradation of dyes from the aqueous solution because the charge transfer resistance is slow, the optimized surface charge and absorption of photons under visible light irradiation is high [86]. Dhirendra Sahoo and colleagues recently showed that MoS_2 nanosheets as grown solid, insoluble (to water and dilute acid), and stable could be used as potential future photocatalytic materials controlling water pollution by degrading hazardous compounds such as methylene blue under the irradiation of visible light due to the possibility of physical adsorption on the surface of MoS_2 [96]. MoS_2 and WS_2 monolayers are currently used for photocatalytic degradation with 2.5 and 2.7 eV electronic bandgap energies. The fresh γ-$CsPbI_3$ NCs/few-layered WS_2 nanosheets display a high photocatalytic degradation efficiency of nearly 100% in 30 min and fully degrade MB into low-weight and low-toxicity inorganic molecules without the formation of any intermediate degradation products due to higher carrier transport properties [97]. Within 120 min under visible-light irradiation, ZnO/WS_2 photocatalyst showed a better degradation efficiency of 95.71% [98]. Flower-like WS_2/BiOBr heterostructure was synthesized, and it was seen that it was very effective for degradation purpose of various toxic dyes and that too with good degradation efficiency as LR5B was degraded up to 99%, MNZ 97%, RhB 90%, and MB 78% [50]. SiO_2/WSe_2-graphene-TiO_2 composite also serves as an excellent photocatalytic agent for cationic organic dyes' degradation by providing a more efficient

hetero system [21]. Amid the hybrid photocatalysts, WSe_2/50NG (50 wt% of NG) showed photocatalytic activity with a rate constant of 0.0572 min-1 (highest) for MB degradation in an aqueous solution because of the strong adsorption of the dye methylene blue [22]. The WSe_2/g-C_3N_4 [23], the CNT/WSe_2 composite [99] reveals higher photocatalytic degradation activity since the charge separation is higher and further leads to the reduced amount of photo-generated electron-hole recombination. High degradation activity under an ultrasonic wave is exhibited by all the TMDs nanosheets, following the order of MoS_2 > WS_2 > WSe_2 [100]. Among the molybdenum series, the maximum amount of dye degradation and that too in the minimum period is shown by flower-like MoS_2, while among the tungsten dichalcogenides, WSe_2 represents the better photocatalytic dye degradation activity. Table 2 depicts the decomposition of various toxic dyes under suitable light irradiation with appropriate and more effective photocatalyst combination with that of metal dichalcogenides. It can be clearly stated that molybdenum sulfides do major dye decomposition. Figure 2 illustrates the schematic view of photocatalytic degradation of methyl red under visible light irradiation. When the sunlight is incident on MoS_2/ZnO heterostructure, both MoS_2 and ZnO get excited, generating e-/h+ pairs. There occurs the shifting of photo-generated electrons towards the more negative CB potential that is from the conduction band of ZnO to that of MoS_2. Adsorbed molecular oxygen (O_2) on capturing the photoexcited e- gets converted to superoxide anion radicals (O^{2-}). The recombination rate of electron-hole pairs is suppressed by the presence of MoS_2, as it captures the electron due to its higher conductivity. The photo-generated holes then react with H_2O or OH^-, giving OH radicals responsible for decomposing toxic dyes [101].

Table 2. *The action of MoS_2 on the decomposition of various toxic organic pollutants under UV-visible light irradiation.*

Serial number	Photocatalyst	Irradiation	Time of Reaction (min)	Dye decomposed	Degradation efficiency (%)	Reference
1.	WS_2 nanosheets	Visible light	40	MB: CR: MO (1:1:1)	>95	[102]
2.	MoS_2 /TiO_2	λ=313 nm	30	Rhodamine B	98.2	[103]
3.	MoS_2 -RGO doped ZnO (1 wt% of MoS_2 -RGO in ZnO)	Natural solar light	60	MB and carbendazim	98 for MB and 97 for carbendazim	[104]
4.	MoS_2/ZnO	Simulated solar light	90	Rhodamine B	91.4	[105]
5.	P-doped ZnO nanosheets decorated MoS_2	Natural solar light	6	MB	95	[106]
6.	MoS_2/ZnO	Natural solar light	20	MB	97	[107]
7.	ZnO-g-C_3N_4 (50%)/MoS_2 (1%)	UV-visible light	30	MB	99.5	[108]
8.	MoS_2 nanosheets/TiO_2 nanobelts	300 W mercury lamp	15	MO	100	[109]
9.	MoS_2 nanodots/TiO_2 NPs	High pressure Hg lamp	20	RhB or MB	100	[110]
10.	Ag_3PO_4/MoS_2	300W Xe arc lamp	8	RhB	90	[111]
11.	MoS_2 nanosheets/TiO_2 nanodrums	250 W Hg lamp	60	MB	70	[112]
12.	MoS_2 nanoflower/TiO_2 nanotube arrays	500 W Xe lamp, λ > 420 nm	180	Levofloxacin	100	[113]
13.	MoS_2 nanobelts/TiO_2 nanotube arrays	500 W Xe lamp, λ ≥ 410 nm	240	Sulfadiazine	64	[114]
14.	Ag_3PO_4 NPs/TiO_2 nanofibers@MoS_2 sheets	800 W Xe lamp	125	MO or MB	>92	[115]
15.	N-TiO_2 NPs/MoS_2 nanosheets	300 W Xe lamp, λ > 400 nm	120	MB	98.5	[116]
16.	N-TiO_2−x nanospheres@MoS_2 nanosheets	300 W Xe lamp, λ > 420 nm	120	MO	91.8	[117]
17.	MoS_2 nanosheets@TiO_2 nanotube array	230 W Hg lamp, λ=365 nm	120	RhB	85.3	[118]
18.	TiO_2-RGO NPs/MoS_2 nanosheets	Sunlight irradiation	100	MB	100	[119]

2.3. Photocatalytic CO_2 Reduction

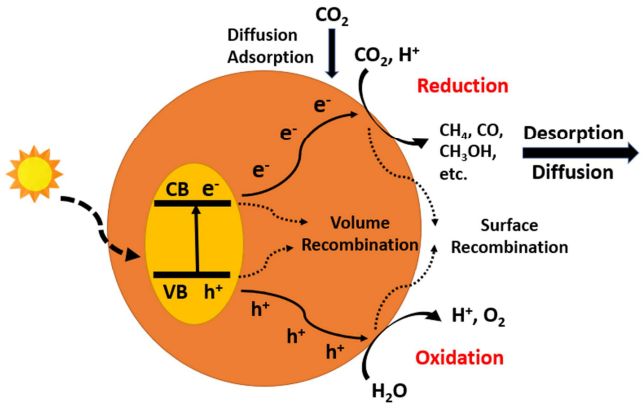

Figure 3. *Photocatalytic CO_2 reduction: The five fundamental steps. [120]*

Carbon dioxide (CO_2) emissions from the burning of fossil fuels contribute to increased greenhouse gas (GHG) levels in the atmosphere. Most countries and scientific research communities' endeavor to solve the climate change issue due to global warming by reducing GHG emissions. To solve the problem of increasing dependency on fossil fuel, replacement with renewable energy is the best solution. Among these potential approaches, the utilization and conversion of CO_2 are preferable since it converts harmful gas into valuable products [121-126]. Figure 3 schematically illustrates a typical process of photocatalytic reduction of carbon dioxide on a semiconductor photocatalyst. They consist of five sequential steps: light absorption, surface redox reaction, product desorption, charge separation, and CO_2 adsorption. TiO_2 is the most widely considered semiconductor photocatalyst, but UV light can only be photo-excited due to its sizeable intrinsic bandgap (3.2 eV). This leaves the visible light unutilized, which counts 46% of the solar spectrum than UV, 3-5% of the entire solar range [127]. Therefore, 2D-TMDCs have gained significant attention regarding their cost-effectiveness, narrow bandgap, and highly visible-light

responsive nano-photocatalysts. MoS_2 and WSe_2 are two family members who have emerged as potential candidates for photocatalytic carbon dioxide reduction. Particularly MoS_2 has strong photocatalytic stability against oxidation compared to other chalcogenides. The exfoliated MoS_2 nanosheets possess physicochemical properties, primarily due to the confinement of charge carriers in their basal plane directions, which are dramatically different from those of the bulk MoS_2. Fabricating hybrid nanocomposites of 2D MoS_2 with different materials, particularly solvent, enhances organic contaminant degradation performance. B. khan et al. recently showed that the nanocomposites of SnO_2/Ag/MoS_2 exhibit exceptional visible-light photocatalytic activities for the conversion of CO_2 to CH_4, approximately one order of magnitude enhancement than original MoS_2 with the apparent quantum efficiency of 2.38% at 420 nm [128]. The appropriate band structure makes MoS_2 nanosheets one of the most promising photocatalyst candidates in environmental fields. A semiconducting photocatalyst can be excited by the photon whose energy exceeds its bandgap energy, and consequently, electrons on the valence band are excited to the conduction band leaving behind holes. These electrons and holes can react with dissolved oxygen and water in separated reactions, forming reactive oxygen species (ROSs) that effectively destroy or mineralize organic contaminants. Such photocatalytic degradation has many advantages, including complete mineralization, low cost, and mild reaction conditions [129-130]. Also, a novel 1D/2D TiO_2/MoS_2 nanostructured hybrid with TiO_2 fibers covered by MoS_2 nanosheets reports photocatalytic CO_2 reduction into methane and methanol [131]. Y. Zheng et al. reported nano-Ag decorated MoS_2 nanosheets through 1 T to 2 H phase conversion for Photocatalytically reducing CO_2 to methanol [132]. M. R. U. D. Biswas et al. reported WSe_2-graphene-TiO_2 ternary nanocomposite giving a yield of 3.80 mmol g^{-1} after 10 hours and 6.63262 µmol g^{-1} h^{-1} after 48 hours [133]. Table 3 demonstrates the reduction of prevalent and harmful gas, carbon dioxide, by applying various metal dichalcogenides. MoS_2 and WSe_2 play a significant role in decomposing CO_2 gas into valuable compounds like methane, methanol, or carbon monoxide gas. Either methanol or methane is usually the primary product.

Table 3. *Photocatalytic carbon dioxide reduction into valuable products by different forms of metal dichalcogenides (MoS_2, WSe_2) under UV-Visible light.*

Serial number	Photocatalyst	Irradiation	Product	Yield (µmol$g^{-1}h^{-1}$)	Reference
1.	2/6/8/-SnO_2/Ag/MoS_2	Visible light	CH_4 CO	14, 15, 12 4, 7, 5	[128]
2.	4SnO_2/Ag/MoS_2	Visible light	CH_4 CO	20 9	[128]
3.	10% MoS_2/TiO_2	350 W Xe lamp	CH_4 CH_3OH	2.86 2.55	[131]
4.	20wt% Ag/2H-MoS_2	250W high-pressure mercury lamp 500 W, SOLAREDGE700	CH_3OH	365.08	[132]
5.	WSe_2-G-TiO_2	UV light Visible light	CH_3OH CH_3OH	5.1244 3.6970	[133]
6.	WSe_2- graphene	Visible light	CH_3OH	3.5509	[25]
7.	WSe_2- graphene+ Na_2SO_3	UV light	CH_3OH	5.0278	[25]

2.4. Other Applications

The carcinogenic wastes and toxic pollutants such as congo red, rhodamine B, and hexavalent chromium (Cr (VI)) are discharged from industries such as textile manufacturing, paints, and pigments, and electroplating has become a severe threat to the environment and the human health [134]. With the global economic growth and the pandemic's current situation, pollutants' treatment has become a global priority. Various methods have been developed for pollutant degradation technologies, such as photocatalytic oxidation, biodegradation, and adsorption. Compared with other technologies, photocatalysis's significant benefits and virtue include the eco-friendly performance due to solar energy, the lack of toxic by-products, and simple reaction conditions. The tuneable bandgap of transition metal dichalcogenides concerning nanosheets' thickness encourages promising future application applications in environmental remediation. 2D-TMDCs: MoS_2, $MoSe_2$, $MoTe_2$, WS_2, WSe_2 based photocatalysts [135-142] have been used for many environmental applications remediation such as organic pollutants degradation like dye degradation in water treatment which already been discussed in detail, and degradation of refractory pollutants. Inorganic pollutants treatment like treatment of heavy metals, Nitric oxide (NO) removal, and the most recent and vital: hexavalent chromium (Cr (VI)) degradation [143-145]. Also, photocatalytic inactivation of microbial pollutants is an extensive research area concerning the use of 2D-TMDCs based photocatalysts because chlorination is the typical conventional disinfection method from many complications. For example, it forms some undesirable disinfection by-products on reaction with natural organic matter, and it is not useful for some pathogens such as protozoa. On the other hand, photocatalytic disinfection is a reusable and green process that does not form DBPs due to its comparatively inert chemical and biological features. In the past decades, the rise in pharmaceutical and personal care products (PPCPs) has raised severe environmental pollution concerns. Leakage of antibiotics, specifically fluoroquinolones (FQs) were used abusively due to their exceptional tissue permeation and broad-spectrum activities. The exposure of FQs in low-concentration for a long term induced toxic effects in several environmental matrices (e.g., water, soil, and sediment) [146]. Most common being ofloxacin (OFL) [147],

ciprofloxacin (CIP) [148], and norfloxacin (NOR) [149]. The wt% WS_2 coating β-Bi_2O_3 photocatalyst exhibited a better removal rate of OFL, CIP, NOR, which were 2.32, 2.01, and 1.71 times greater than those of β-Bi_2O_3 under similar conditions [150]. This also led to the inception and spread of antibiotic-resistant bacteria and genes, which is alarming if considered in the present time. R. A. Senthil et al. have offered $BiFeWO_6/MoS_2$ composite as a potential photocatalyst to eliminate organic contaminants from wastewater [151]. W. Ashraf et al. and S. Fu et al. have recently reported $BiOCl/WS_2$ hybrid nanosheet (2D/2D) heterojunctions for visible-light-driven photocatalytic degradation of organic/inorganic water pollutants and WS_2/BiOBr heterojunction for photodegradation of several organic pollutants, such as ciprofloxacin (CIP), tetracycline (TC), oxytetracycline (OTC), Rhodamine B (RhB), methyl orange (MO), and methylene blue (MB) respectively [152-153].

3. Conclusions and Future Perspectives

In the past decade, the compound that has emerged as a promising candidate among researchers struggling with the semi-metallic zero-bandgap graphene is MoS_2. It is so much discussed in the literature that we tend to focus on the other family members in our review, which are equally important and efficient as far as the applications are concerned. $MoSe_2$ is one such member that is used widely in the field of optoelectronics due to its versatile bandgap. However, the photocatalytic application's performance is also promising, mainly by controlling or doping the product, enhancing its properties. In the common TMDCs, Tungsten being the largest atom provides an opportunity to form more spacious interlayer channels. This manuscript attempted to highlight the popular molybdenum dichalcogenides and the tungsten dichalcogenides by collecting the noticeable findings reported in the literature during the past few years. The development of which clearly shows the promising future ahead for tungsten dichalcogenides. Developing novel methods should be the focus for WX_2 (X=S, Se) materials because several exfoliation methods have been developed and tested for more common TMDCs such as MoS_2. However, these methods do not seem efficient for WX_2 (X=S, Se) because of differences in the lattice structure and chemical reactivity. Simplistic and scalable production of large-sized monolayer nanosheets should be prioritized because it is the most severe challenge in many of these applications, particularly those based on light-matter interaction. In the realm of layered 2D-TMDCs, there are many opportunities and uncharted areas, and the sky is the limit. We sincerely hope this review will give a defining perspective and add new dimensions to understanding this subject. This rapidly growing research field will also encourage innovation and ignite novel ideas to uplift further progress.

Conflict of Interest

There is no conflict of any type between the authors.

References

[1] Ali, M. N., Xiong, J., Flynn, S., Tao, J., Gibson, Q. D., Schoop, L. M., & Cava, R. J. (2014). Large, non-saturating magnetoresistance in WTe_2. *Nature*, *514* (7521), 205-208. https://doi.org/10.1038/nature13763.

[2] Duan, X., Wang, C., Pan, A., Yu, R., & Duan, X. (2015). Two-dimensional transition metal dichalcogenides as atomically thin semiconductors: opportunities and challenges. *Chemical Society Reviews*, *44* (24), 8859-8876. https://doi.org/10.1039/C5CS00507H.

[3] Huang, X., Zeng, Z., & Zhang, H. (2013). Metal dichalcogenide nanosheets: preparation, properties and applications. *Chemical Society Reviews*, *42* (5), 1934-1946. https://doi.org/10.1039/C2CS35387C.

[4] Low, J., Cao, S., Yu, J., & Wageh, S. (2014). Two-dimensional layered composite photocatalysts. *Chemical communications*, *50* (74), 10768-10777. https://doi.org/10.1039/C4CC02553A.

[5] Wang, F., Shifa, T. A., Zhan, X., Huang, Y., Liu, K., Cheng, Z., & He, J. (2015). Recent advances in transition-metal dichalcogenide based nanomaterials for water splitting. *Nanoscale*, *7* (47), 19764-19788. https://doi.org/10.1039/C5NR06718A.

[6] Ozdemir, B., & Barone, V. (2020). Thickness dependence of solar cell efficiency in transition metal dichalcogenides MX_2 (M: Mo, W; X: S, Se, Te). *Solar Energy Materials and Solar Cells*, *212*, 110557. https://doi.org/10.1016/j.solmat.2020.110557.

[7] Naidu, K. C. B., Kumar, N. S., Boddula, R., Pothu, R., Banerjee, P., Sarma, M. S. S. R. K. N, & Kishore, B. (2020). Recent Advances in Nanomaterials for Li-ion Batteries. *Lithium-ion Batteries: Materials and Applications*, *80*, 148-160. https://doi.org/10.21741/9781644900918-6.

[8] Choi, W., Akhtar, I., Kang, D., Lee, Y. J., Jung, J., Kim, Y. H. & Seo, Y. (2020). Optoelectronics of Multijunction Heterostructures of Transition Metal Dichalcogenides. *Nano Letters*, *20* (3), 1934-1943. https://doi.org/10.1021/acs.nanolett.9b05212.

[9] Kannan, P. K., Late, D. J., Morgan, H., & Rout, C. S. (2015). Recent developments in 2D layered inorganic nanomaterials for sensing. *Nanoscale*, *7* (32), 13293-13312. https://doi.org/10.1039/C5NR03633J.

[10] Huang, Y., Guo, J., Kang, Y., Ai, Y., & Li, C. M. (2015). Two dimensional atomically thin MoS_2 nanosheets and their sensing applications. *Nanoscale*, *7* (46), 19358-19376. https://doi.org/10.1039/C5NR06144J.

[11] Brent, J. R., Savjani, N., & O'Brien, P. (2017). Synthetic approaches to two-dimensional transition metal dichalcogenide nanosheets. *Progress in Materials Science*, *89*, 411-478. https://doi.org/10.1016/j.pmatsci.2017.06.002.

[12] Eftekhari, A. (2017). Tungsten dichalcogenides (WS_2, WSe_2, and WTe_2): materials chemistry and applications. *Journal of Materials Chemistry A*, *5* (35), 18299-18325. https://doi.org/10.1039/C7TA04268J.

[13] Krishnan, U., Kaur, M., Singh, K., Kumar, M., & Kumar, A. (2019). A synoptic review of MoS_2: Synthesis to applications. *Superlattices and Microstructures*, *128*, 274-297. https://doi.org/10.1016/j.spmi.2019.02.005.

[14] Kaur, M., Umar, A., Mehta, S. K., Singh, S., & Kansal, S. K. (2017). Visible-light photocatalytic degradation of organic pollutants using molybdenum disulfide (MoS_2) microtubes. *Nanoscience and Nanotechnology Letters*, *9* (12), 1966-1974. https://doi.org/10.1166/nnl.2017.2591.

[15] Ren, B., Shen, W., Li, L., Wu, S., & Wang, W. (2018). 3D $CoFe_2O_4$ nanorod/flower-like MoS_2 nanosheet heterojunctions as recyclable visible light-driven photocatalysts for the degradation of organic dyes. *Applied Surface Science*, *447*, 711-723. https://doi.org/10.1016/j.apsusc.2018.04.064.

[16] Liang, Z., Shen, R., Ng, Y. H., Zhang, P., Xiang, Q., & Li, X. (2020). A review on 2D MoS_2 co-catalysts in photocatalytic H_2 production. *Journal of Materials Science & Technology*. https://doi.org/10.1039/D0TA08045D.

[17] Zhang, Y., Liu, Y., Gao, W., Chen, P., Cui, H., Fan, Y., & Tang, B. (2019). MoS_2 nanosheets assembled on three-way nitrogen-doped carbon tubes for photocatalytic water splitting. *Frontiers in Chemistry*, *7*, 325. https://doi.org/10.3389/fchem.2019.00325.

[18] Liu, P., Zhu, J., Zhang, J., Tao, K., Gao, D., & Xi, P. (2018). Active basal plane catalytic activity and conductivity in Zn doped MoS_2 nanosheets for efficient hydrogen evolution. *Electrochimica Acta*, *260*, 24-30. https://doi.org/10.1016/j.electacta.2017.11.080.

[19] Kou, S., Guo, X., Xu, X., & Yang, J. (2018). TiO_2 on $MoSe_2$ nanosheets as an advanced photocatalyst for hydrogen evolution in visible light. *Catalysis Communications*, *106*, 60-63. https://doi.org/10.1016/j.catcom.2017.12.013.

[20] Lei, W., Xiao, J. L., Liu, H. P., Jia, Q. L., & Zhang, H. J. (2020). Tungsten disulfide: synthesis and applications in electrochemical energy storage and conversion. *Tungsten*, 1-23. https://doi.org/10.1007/s42864-020-00054-6.

[21] Zhu, L., Nguyen, D. C. T., Woo, J. H., Zhang, Q., Cho, K. Y., & Oh, W. C. (2018). An eco-friendly synthesized mesoporous-silica particle combined with WSe_2-graphene-TiO_2 by self-assembled method for photocatalytic dye decomposition and hydrogen production. *Scientific reports*, *8* (1), 1-14. https://doi.org/10.1038/s41598-018-31188-w.

[22] Wan, J., An, B., Chen, Z., Zhang, J., & William, W. Y. (2018). Nitrogen doped graphene oxide modified WSe_2 nanorods for visible light photocatalysis. *Journal of Alloys and Compounds*, *750*, 499-506. https://doi.org/10.1016/j.jallcom.2018.04.047.

[23] Yu, B., Zheng, B., Wang, X., Qi, F., He, J., Zhang, W., & Chen, Y. (2017). Enhanced photocatalytic properties of graphene modified few-layered WSe_2 nanosheets. *Applied Surface Science*, *400*, 420-425. https://doi.org/10.1016/j.apsusc.2016.12.015.

[24] An, B., Liu, Y., Xu, C., Wang, H., & Wan, J. (2018). Novel magnetically separable Fe_3O_4–WSe_2/NG photocatalysts: synthesis and photocatalytic performance under visible-light irradiation. *New Journal of Chemistry*, *42* (11), 8914-8923. https://doi.org/10.1039/C8NJ00406D.

[25] Ali, A., & Oh, W. C. (2017). Preparation of nanowire like WSe_2-graphene nanocomposite for photocatalytic reduction of CO_2 into CH_3OH with the presence of sacrificial agents. *Scientific Reports*, *7* (1), 1-11. https://doi.org/10.1038/s41598-017-02075-7.

[26] Zhong, Y., Shao, Y., Ma, F., Wu, Y., Huang, B., & Hao, X. (2017). Band-gap-matched CdSe QD/WS_2 nanosheet composite: Size-controlled photocatalyst for high-efficiency water splitting. *Nano Energy*, *31*, 84-89. https://doi.org/10.1016/j.nanoen.2016.11.011.

[27] Wang X, Cao Z, Zhang Y, Xu H, Cao S, Zhang R. All-solid-state Z-scheme Pt/ZnS-ZnO heterostructure sheets for photocatalytic simultaneous evolution of H_2 and O_2. Chem Eng J 2020; 385: 123782. https://doi.org/10.1016/j.cej.2019.123782.

[28] Li, S., Lei, F. C., Peng, X., Wang, R. Q., Xie, J. F., Wu, Y. P., & Li, D. S. (2020). Synthesis of Semiconducting 2H-Phase WTe_2 Nanosheets with Large Positive Magnetoresistance. *Inorganic Chemistry*, *59* (17), 11935-11939. https://doi.org/10.1021/acs.inorgchem.0c02049.

[29] Ping, J., Fan, Z., Sindoro, M., Ying, Y., & Zhang, H. (2017). Recent advances in sensing applications of two-dimensional transition metal dichalcogenide nanosheets and their composites. *Advanced Functional Materials*, *27* (19), 1605817.Eftekhari, A. (2017). Tungsten dichalcogenides (WS_2, WSe_2, and WTe_2): materials chemistry and applications. *Journal of Materials Chemistry A*, *5* (35), 18299-18325. https://doi.org/10.1002/adfm.201605817.

[30] Wu, M., Xiao, Y., Zeng, Y., Zhou, Y., Zeng, X., Zhang, L., & Liao, W. (2020). Synthesis of two-dimensional transition metal dichalcogenides for electronics and optoelectronics. *InfoMat*. https://doi.org/10.1002/inf2.12161.

[31] Chhowalla, M., Shin, H. S., Eda, G., Li, L. J., Loh, K. P., & Zhang, H. (2013). The chemistry of two-dimensional layered transition metal dichalcogenide nanosheets. *Nature chemistry*, *5* (4), 263-275. https://doi.org/10.1038/nchem.1589.

[32] Samadi, M., Sarikhani, N., Zirak, M., Zhang, H., Zhang, H. L., & Moshfegh, A. Z. (2018). Group 6 transition metal dichalcogenide nanomaterials: synthesis, applications and future perspectives. *Nanoscale Horizons*, *3* (2), 90-204. https://doi.org/10.1039/C7NH00137A.

[33] Wang, K., Li, Y., Li, J., & Zhang, G. (2020). Boosting interfacial charge separation of $Ba_5Nb_4O_{15}$/g-C_3N_4 photocatalysts by 2D/2D nanojunction towards efficient visible-light driven H_2 generation. *Applied Catalysis B: Environmental*, *263*, 117730. https://doi.org/10.1016/j.apcatb.2019.05.032.

[34] Shi, X., Kim, S., Fujitsuka, M., & Majima, T. (2019). In situ observation of NiS nanoparticles depositing on single TiO_2 mesocrystal for enhanced photocatalytic hydrogen evolution activity. *Applied Catalysis B: Environmental*, *254*, 594-600. https://doi.org/10.1016/j.apcatb.2019.05.031.

[35] Hisatomi, T., Kubota, J., & Domen, K. (2014). Recent advances in semiconductors for photocatalytic and photoelectrochemical water splitting. *Chemical Society Reviews*, *43* (22), 7520-7535. https://doi.org/10.1039/C3CS60378D.

[36] Moniz, S. J., Shevlin, S. A., Martin, D. J., Guo, Z. X., & Tang, J. (2015). Visible-light driven heterojunction photocatalysts for water splitting–a critical review. *Energy & Environmental Science*, *8* (3), 731-759. https://doi.org/10.1039/C4EE03271C.

[37] Li, M., Cui, Z., & Li, E. (2019). Silver-modified MoS_2 nanosheets as a high-efficiency visible-light photocatalyst for water splitting. *Ceramics International*, *45* (11), 14449-14456. https://doi.org/10.1016/j.ceramint.2019.04.166.

[38] C. Dai, E. Qing, Y. Li, Z. Zhou & C. Yang, Novel $MoSe_2$ hierarchical microspheres for applications in visible-light-driven advanced oxidation processes, *Nanoscale* 7 (2015) 19970–19976. https://doi.org/10.1039/C5NR06527E.

[39] Y. Sang, Z. Zhao, M. Zhao, P. Hao, Y. Leng, H. Liu, From UV to near-Infrared, WS_2 nanosheet: a novel photocatalyst for full solar light spectrum photodegradation, *Adv. Mater.* 27 (2015) 363–369. https://doi.org/10.1002/adma.201403264.

[40] Luo, B., Liu, G., & Wang, L. (2016). Recent advances in 2D materials for photocatalysis. *Nanoscale*, *8* (13), 6904-6920. https://doi.org/10.1039/C6NR00546B.

[41] Z. Liu, H. Zhao, N. Li, Y. Zhang, X. Zhang, Y. Du, assembled 3D electrocatalysts for efficient hydrogen evolution: WSe_2 layers anchored on graphene sheets, Inorg. Chem. 3 (2016) 313–319. https://doi.org/10.1039/C5QI00216H.

[42] He, H. Y., He, Z., & Shen, Q. (2018). Efficient hydrogen evolution catalytic activity of graphene/metallic MoS_2 nanosheet heterostructures synthesized by a one-step hydrothermal process. *International Journal of Hydrogen Energy*, *43* (48), 21835-21843. https://doi.org/10.1016/j.ijhydene.2018.10.023.

[43] Ma, F., Wu, Y., Shao, Y., Zhong, Y., Lv, J., & Hao, X. (2016). 0D/2D nanocomposite visible light photocatalyst for highly stable and efficient hydrogen generation via recrystallization of CdS on MoS_2 nanosheets. *Nano Energy*, *27*, 466-474. https://doi.org/10.1002/adma.201605646.

[44] Chava, R. K., Do, J. Y., & Kang, M. (2018). Smart hybridization of Au coupled CdS nanorods with few layered MoS_2 nanosheets for high performance photocatalytic hydrogen evolution reaction. *ACS Sustainable Chemistry & Engineering*, *6* (5), 6445-6457. https://doi.org/10.1021/acssuschemeng.8b00249.

[45] Reddy, D. A., Kim, E. H., Gopannagari, M., Kim, Y., Kumar, D. P., & Kim, T. K. (2019). Few layered black phosphorus/MoS_2 nanohybrid: a promising co-catalyst for solar driven hydrogen evolution. *Applied Catalysis B: Environmental*, *241*, 491-498. https://doi.org/10.1016/j.apcatb.2018.09.055.

[46] Reddy, D. A., Park, H., Ma, R., Kumar, D. P., Lim, M., & Kim, T. K. (2017). Heterostructured WS_2-MoS_2 Ultrathin Nanosheets Integrated on CdS Nanorods to Promote Charge Separation and Migration and Improve Solar-Driven Photocatalytic Hydrogen Evolution. *ChemSusChem*, *10* (7), 1563-1570. https://doi.org/10.1002/cssc.201601799.

[47] Yuan, Y. J., Shen, Z., Wu, S., Su, Y., Pei, L., Ji, Z. & Zou, Z. (2019). Liquid exfoliation of g-C_3N_4 nanosheets to construct 2D-2D MoS_2/g-C_3N_4 photocatalyst for enhanced photocatalytic H2 production activity. *Applied Catalysis B: Environmental*, *246*, 120-128. https://doi.org/10.1016/j.cej.2020.127804.

[48] Li, Y., Zhang, P., Wan, D., Xue, C., Zhao, J., & Shao, G. (2020). Direct evidence of 2D/1D heterojunction enhancement on photocatalytic activity through assembling MoS_2 nanosheets onto super-long TiO_2 nanofibers. *Applied Surface Science*, *504*, 144361. https://doi.org/10.1016/j.apsusc.2019.144361.

[49] Zhang, J., Tian, P., Tang, T., Huang, G., Chen, X., Zeng, J. & Ji, Z. (2020). Ultrathin $MoSe_2$ three-dimensional nanospheres as high carriers transmission channel and full spectrum harvester toward excellent photocatalytic and photoelectrochemical performance. *International Journal of Hydrogen Energy*, *45* (11), 6519-6528. https://doi.org/10.1016/j.ijhydene.2019.12.217.

[50] Wang, Y., Zhao, J., Chen, Z., Zhang, F., Guo, W., Lin, H., & Qu, F. (2019). Construction of Z-scheme $MoSe_2$/CdSe hollow nanostructure with enhanced full spectrum photocatalytic activity. *Applied Catalysis B: Environmental*, *244*, 76-86. https://doi.org/10.1016/j.apcatb.2018.11.033.

[51] Mak, K. F., & Shan, J. (2016). Photonics and optoelectronics of 2D semiconductor transition metal dichalcogenides. *Nature Photonics*, *10* (4), 216-226. https://doi.org/10.1038/nphoton.2015.282.

[52] Wu, L., Shi, S., Li, Q., Zhang, X., & Cui, X. (2019). TiO_2 nanoparticles modified with 2D $MoSe_2$ for enhanced photocatalytic activity on hydrogen evolution. *International Journal of Hydrogen Energy*, *44* (2), 720-728. https://doi.org/10.1016/j.ijhydene.2018.10.214.

[53] Fan, C., Wei, Z., Yang, S., & Li, J. (2014). Synthesis of MoSe2 flower-like nanostructures and their photo-responsive properties. *RSC Advances*, *4* (2), 775-778. https://doi.org/10.1039/C3RA42564A.

[54] Choi, W., Choudhary, N., Han, G. H., Park, J., Akinwande, D., & Lee, Y. H. (2017). Recent development of two-dimensional transition metal dichalcogenides and their applications. *Materials Today*, *20* (3), 116-130. https://doi.org/10.1016/j.mattod.2016.10.002.

[55] Zeng, D., Xiao, L., Ong, W. J., Wu, P., Zheng, H., Chen, Y., & Peng, D. L. (2017). Hierarchical $ZnIn_2S_4$/$MoSe_2$ Nanoarchitectures for Efficient Noble-Metal-Free Photocatalytic Hydrogen Evolution under Visible Light. *ChemSusChem*, *10* (22), 4624-4631. https://doi.org/10.1002/cssc.201701345.

[56] Masih, D., Ma, Y., & Rohani, S. (2017). Graphitic C_3N_4 based noble-metal-free photocatalyst systems: a review. *Applied Catalysis B: Environmental*, *206*, 556-588. https://doi.org/10.1016/j.apcatb.2017.01.061.

[57] Liu, Y., Li, Y., Lin, Y., Yang, S., Zhang, Q., & Peng, F. (2020). Theoretical calculations and controllable synthesis of $MoSe_2$/CdS-CdSe with highly active sites for photocatalytic hydrogen evolution. *Chemical Engineering Journal*, *383*, 123133. https://doi.org/10.1016/j.cej.2019.123133.

[58] Mao, J., Zhou, L., Li, Y., Tao, Y., Chai, K., Shi, Y., & Xu, W. (2021). Synthesis of $MoTe_2$ nanowire as an efficient hydrogen evolution reaction material. *Materials Letters*, 129471. https://doi.org/10.1016/j.matlet.2021.129471.

[59] Kang, J., Tongay, S., Zhou, J., Li, J., & Wu, J. (2013). Band offsets and heterostructures of two-dimensional semiconductors. *Applied Physics Letters*, *102* (1), 012111. https://doi.org/10.1063/1.4774090.

[60] He, H. Y., He, Z., & Shen, Q. (2020). One-pot synthesis of non-precious metal RGO/1T'-$MoTe_2$: Cu heterohybrids for excellent catalytic hydrogen evolution. *Materials Science and Engineering: B*, *260*, 114659. https://doi.org/10.1016/j.mseb.2020.114659.

[61] Xu, D., Xu, P., Zhu, Y., Peng, W., Li, Y., Zhang, G., & Fan, X. (2018). High yield exfoliation of WS_2 crystals into 1–2 layer semiconducting nanosheets and efficient photocatalytic hydrogen evolution from WS_2/CdS nanorod composites. *ACS applied materials & interfaces*, *10* (3), 2810-2818. https://doi.org/10.1021/acsami.7b15614.

[62] Zhang, K., Fujitsuka, M., Du, Y., & Majima, T. (2018). 2D/2D heterostructured CdS/WS_2 with efficient charge separation improving H_2 evolution under visible light irradiation. *ACS applied materials & interfaces*, *10* (24), 20458-20466. https://doi.org/10.1021/acsami.8b04080.

[63] Akple, M. S., Low, J., Wageh, S., Al-Ghamdi, A. A., Yu, J., & Zhang, J. (2015). Enhanced visible light photocatalytic H_2-production of g-C_3N_4/WS_2 composite heterostructures. *Applied Surface Science*, *358*, 196-203. https://doi.org/10.1016/j.apsusc.2015.08.250.

[64] Wang, X., Chen, Y., Zheng, B., Qi, F., He, J., Li, Q, & Zhang, W. (2017). Graphene-like WSe_2 nanosheets for efficient and stable hydrogen evolution. *Journal of Alloys and Compounds*, *691*, 698-704. https://doi.org/10.1016/j.jallcom.2016.08.305.

[65] He, H. Y. (2020). Metallic WSe_2: Sn nanosheets assembled on graphene by a modified hydrothermal process for hydrogen evolution reaction. *Colloids and Surfaces A: Physicochemical and Engineering Aspects*, *589*, 124149. https://doi.org/10.1016/j.colsurfa.2019.124149.

[66] Xu, M., Wei, Z., Liu, J., Guo, W., Zhu, Y., Chi, J.,... & Shangguan, W. (2019). One-pot synthesized visible-light-responsive MoS_2@ CdS nanosheets-on-nanospheres for hydrogen evolution from the antibiotic wastewater: Waste to energy insight. *International Journal of Hydrogen Energy*, *44* (39), 21577-21587. https://doi.org/10.1016/j.ijhydene.2019.06.082.

[67] Min, S., & Lu, G. (2012). Sites for high efficient photocatalytic hydrogen evolution on a limited-layered MoS_2 cocatalyst confined on graphene sheets—the role of graphene. *The Journal of Physical Chemistry C*, *116* (48), 25415-25424. https://doi.org/10.1021/jp3093786.

[68] Maitra, U., Gupta, U., De, M., Datta, R., Govindaraj, A., & Rao, C. N. R. (2013). Highly effective visible-light-induced H_2 generation by single-layer 1T-MoS_2 and a nanocomposite of few-layer 2H-MoS_2 with heavily nitrogenated graphene. *Angewandte Chemie International Edition*, *52* (49), 13057-13061. https://doi.org/10.1002/anie.201306918.

[69] Gupta, U., & Rao, C. N. R. (2017). Hydrogen generation by water splitting using MoS_2 and other transition metal dichalcogenides. *Nano Energy*, *41*, 49-65. http://dx.doi.org/10.1016/j.nanoen.2017.08.021.

[70] Liu, M., Li, F., Sun, Z., Ma, L., Xu, L., & Wang, Y. (2014). Noble-metal-free photocatalysts MoS_2–graphene/CdS mixed nanoparticles/nanorods morphology with high visible light efficiency for H_2 evolution. *Chemical Communications*, *50* (75), 11004-11007. https://doi.org/10.1039/C4CC04653F.

[71] Zong, X., Han, J., Ma, G., Yan, H., Wu, G., & Li, C. (2011). Photocatalytic H_2 evolution on CdS loaded with WS_2 as cocatalyst under visible light irradiation. *The Journal of Physical Chemistry C*, *115* (24), 12202-12208. https://doi.org/10.1021/jp2006777.

[72] Mahler, B., Hoepfner, V., Liao, K., & Ozin, G. A. (2014). Colloidal synthesis of 1T-WS_2 and 2H-WS_2 nanosheets: applications for photocatalytic hydrogen evolution. *Journal of the American Chemical Society*, *136* (40), 14121-14127. https://doi.org/10.1021/ja506261t.

[73] Xiang, Q., Yu, J., & Jaroniec, M. (2012). Synergetic effect of MoS_2 and graphene as cocatalysts for enhanced photocatalytic H_2 production activity of TiO_2 nanoparticles. *Journal of the American Chemical Society*, *134* (15), 6575-6578. https://doi.org/10.1021/ja302846n.

[74] Meng, F., Li, J., Cushing, S. K., Zhi, M., & Wu, N. (2013). Solar hydrogen generation by nanoscale p–n junction of p-type molybdenum disulfide/n-type nitrogen-doped reduced graphene oxide. *Journal of the American Chemical Society*, *135* (28), 10286-10289. https://doi.org/10.1021/ja404851s.

[75] Zeng, D., Wu, P., Ong, W. J., Tang, B., Wu, M., Zheng, H.,... & Peng, D. L. (2018). Construction of network-like and flower-like 2H-$MoSe_2$ nanostructures coupled with porous g-C_3N_4 for noble-metal-free photocatalytic H_2 evolution under visible light. *Applied Catalysis B: Environmental*, *233*, 26-34. https://doi.org/10.1016/j.apcatb.2018.03.102.

[76] Wu, L., Li, Q., Yang, C., Chen, Y., Dai, Z., Yao, B.,... & Cui, X. (2020). Ternary TiO_2/$MoSe_2$/γ-graphyne heterojunctions with enhanced photocatalytic hydrogen evolution. *Journal of Materials Science: Materials in Electronics*, *31* (11), 8796-8804. https://doi.org/10.1007/s10854-020-03414-7.

[77] Cheah, A. J., Chiu, W. S., Khiew, P. S., Nakajima, H., Saisopa, T., Songsiriritthigul, P., & Hamid, M. A. A. (2015). Facile synthesis of a Ag/MoS_2 nanocomposite photocatalyst for enhanced visible-light driven hydrogen gas evolution. *Catalysis Science & Technology*, *5* (8), 4133-4143. https://doi.org/10.1039/C5CY00464K.

[78] Choi, J., Reddy, D. A., Han, N. S., Jeong, S., Hong, S., Kumar, D. P.,.. & Kim, T. K. (2017). Modulation of charge carrier pathways in CdS nanospheres by integrating MoS_2 and Ni_2P for improved migration and separation toward enhanced photocatalytic hydrogen evolution. *Catalysis Science & Technology*, *7* (3), 641-649. https://doi.org/10.1039/C6CY02145J.

[79] Wang, M., Ju, P., Zhao, Y., Li, J., Han, X., & Hao, Z. (2018). In situ ion exchange synthesis of MoS_2/gC_3N_4 heterojunctions for highly efficient hydrogen production. *New Journal of Chemistry*, *42* (2), 910-917. https://doi.org/10.1039/C7NJ03483K.

[80] Wan, J., Wang, R., Liu, L., Fan, J., Liu, E., Gao, X., & Fu, F. (2019). A novel approach for high-yield solid few-layer MoS_2 nanosheets with effective photocatalytic hydrogen evolution. *International Journal of Hydrogen Energy*, *44* (31), 16639-16647. https://doi.org/10.1016/j.ijhydene.2019.04.150.

[81] Sharma, R., Khanuja, M., Islam, S. S., Singhal, U., & Varma, A. (2017). Aspect-ratio-dependent photoinduced antimicrobial and photocatalytic organic pollutant degradation efficiency of ZnO nanorods. *Research on Chemical Intermediates*, *43* (10), 5345-5364. https://doi.org/10.1007/s11164-017-2930-7.

[82] Pu, Y. C., Chen, Y. C., & Hsu, Y. J. (2010). Au-decorated Na_xH_2− xTi_3O_7 nanobelts exhibiting remarkable photocatalytic properties under visible-light illumination. *Applied Catalysis B: Environmental*, *97* (3-4), 389-397. https://doi.org/10.1016/j.apcatb.2010.04.023.

[83] Kumar, A., Singh, S., & Khanuja, M. (2020). A comparative photocatalytic study of pure and acid-etched template free graphitic C_3N_4 on different dyes: An investigation on the influence of surface modifications. *Materials Chemistry and Physics*, *243*, 122402. https://doi.org/10.1016/j.matchemphys.2019.122402.

[84] Ansari, M. Z., Ansari, S. A., Parveen, N., Cho, M. H., & Song, T. (2018). Lithium-ion storage ability, supercapacitor electrode performance, and photocatalytic performance of tungsten disulfide nanosheets. *New Journal of Chemistry*, *42* (8), 5859-5867. https://doi.org/10.1039/C8NJ00018B.

[85] Ntakadzeni, M., Anku, W. W., Kumar, N., Govender, P. P., & Reddy, L. (2019). PEGylated MoS_2 nanosheets: A dual functional photocatalyst for photodegradation of organic dyes and photoreduction of chromium from aqueous solution. *Bulletin of Chemical Reaction Engineering & Catalysis*, *14* (1), 142-152. https://doi.org/10.9767/bcrec.14.1.2258.142-152.

[86] Mittal, H., & Khanuja, M. Hydrothermal in-situ synthesis of $MoSe_2$-polypyrrole nanocomposite for efficient photocatalytic degradation of dyes under dark and visible light irradiation. *Separation and Purification Technology*, *254*, 117508. https://doi.org/10.1016/j.seppur.2020.117508.

[87] Li, P. H., Chen, L,. Zhang, Y., Ji, X. R., Chen, S., Song, H. J., Li, C. S. & H. Tang, Synthesis of $MoSe_2$/reduced graphene oxide composites with improved tribological properties for oil-based additives, Cryst. Res. Technol. 49 (2014) 204–211. https://doi.org/10.1002/crat.201300317.

[88] Wu, Y., Xu, M., Chen, X. S., Yang, H. Wu, Pan, J. & Xiong, X. CTAB-assisted synthesis of novel ultrathin $MoSe_2$ nanosheets perpendicular to graphene for the adsorption and photodegradation of organic dyes under visible light, Nanoscale 8 (2016) 440–450. https://doi.org/10.1039/C5NR05748E.

[89] B. Yu, B. Zheng, X. Wang, F. Qi, J. He, W. Zhang & Y. Chen, Enhanced photocatalytic properties of graphene modified few-layered WSe_2 nanosheets, Appl. Surf. Sci. 400 (2017) 420–425. https://doi.org/10.1016/j.apsusc.2016.12.015.

[90] Rani, A., Patel, A. S., Chakraborti, A., Singh, K., & Sharma, P. (2021). Enhanced photocatalytic activity of plasmonic Au nanoparticles incorporated MoS_2 nanosheets for degradation of organic dyes. *Journal of Materials Science: Materials in Electronics*, 1-17. https://arxiv.org/abs/2006.16211.

[91] Li, Y., Xiang, F., Lou, W., & Zhang, X. (2019, July). MoS_2 with structure tuned photocatalytic ability for degradation of methylene blue. In *IOP Conference Series: Earth and Environmental Science* (Vol. 300, No. 5, p. 052021). IOP Publishing. https://doi.org/10.1088/1755-1315/300/5/052021.

[92] Huang, J., Jin, B., Liu, H., Li, X., Zhang, Q., Chu, S.,... & Chu, S. (2018). Controllable synthesis of flower-like $MoSe_2$ 3D microspheres for highly efficient visible-light photocatalytic degradation of nitro-aromatic explosives. *Journal of Materials Chemistry A*, *6* (24), 11424-11434. https://doi.org/10.1039/C8TA02287A.

[93] Lei, X., Yu, K., Tang, Z., & Zhu, Z. (2017). Synthesized $MoSe_2/TiO_2$ heterogeneous structure as the promising photocatalytic material: Studies from theory to experiment. *Journal of Applied Physics*, *121* (4), 044303. https://doi.org/10.1063/1.4974911.

[94] Mittal, H., Kumar, A., & Khanuja, M. (2019). In-situ oxidative polymerization of aniline on hydrothermally synthesized $MoSe_2$ for enhanced photocatalytic degradation of organic dyes. *Journal of Saudi Chemical Society*, *23* (7), 836-845. https://doi.org/10.1016/j.jscs.2019.02.004.

[95] Tsai, C., Chan, K., Abild-Pedersen, F., & Nørskov, J. K. (2014). Active edge sites in $MoSe_2$ and WSe_2 catalysts for the hydrogen evolution reaction: a density functional study. *Physical Chemistry Chemical Physics*, *16* (26), 13156-13164. https://doi.org/10.1039/C4CP01237B.

[96] Dhirendra, S., Kumar, B., Jaivardhan, S., Subhasis, G., Sinha, R. S., & Bhaskar, K. (2020). Cost effective liquid phase exfoliation of MoS_2 nanosheets and photocatalytic activity for wastewater treatment enforced by visible light. *Scientific Reports (Nature Publisher Group)*, *10* (1). https://doi.org/10.1038/s41598-020-67683-2.

[97] Zhang, Q., Tai, M., Zhou, Y., Zhou, Y., Wei, Y., Tan, C. & Lin, H. (2019). Enhanced photocatalytic property of γ-$CsPbI_3$ perovskite nanocrystals with WS_2. *ACS Sustainable Chemistry & Engineering*, *8* (2), 1219-1229. https://doi.org/10.1021/acssuschemeng.9b06451.

[98] Zhang, X., Qiu, F., Rong, X., Xu, J., Rong, J., & Zhang, T. (2018). Zinc oxide/graphene-like tungsten disulphide nanosheet photocatalysts: Synthesis and enhanced photocatalytic activity under visible-light irradiation. *The Canadian Journal of Chemical Engineering*, *96* (5), 1053-1061. https://doi.org/10.1002/cjce.23039.

[99] Wang, X., Chen, Y., Zheng, B., Qi, F., He, J., Yu, B., & Zhang, W. (2017). Significant enhancement of photocatalytic activity of multi-walled carbon nanotubes modified WSe_2 composite. *Materials Letters*, *197*, 67-70. https://doi.org/10.1016/j.matlet.2017.03.150.

[100] Li, S., Zhao, Z., Yu, D., Zhao, J. Z., Su, Y., Liu, Y.,... & Zhang, Z. (2019). Few-layer transition metal dichalcogenides (MoS_2, WS_2, and WSe_2) for water splitting and degradation of organic pollutants: Understanding the piezocatalytic effect. *Nano Energy*, *66*, 104083. https://doi.org/10.1016/j.nanoen.2019.104083.

[101] Kaur, A., Umar, A., Anderson, W. A., & Kansal, S. K. (2018). Facile synthesis of CdS/TiO_2 nanocomposite and their catalytic activity for ofloxacin degradation under visible illumination. *Journal of Photochemistry and Photobiology A: Chemistry*, *360*, 34-43. https://doi.org/10.1016/j.jphotochem.2018.04.021.

[102] Patel, M., Patel, M. H., & Sumesh, C. K. (2020, May). Visible light enhanced photocatalytic performance of WS2 catalyst for the degradation of ternary dye mixture. In *AIP Conference Proceedings* (Vol. 2220, No. 1, p. 020047). AIP Publishing LLC. https://doi.org/10.1063/5.0001154.

[103] Zhang, J., Huang, L., Lu, Z., Jin, Z., Wang, X., Xu, G.,... & Ji, Z. (2016). Crystal face regulating MoS_2/TiO_2 (001) heterostructure for high photocatalytic activity. *Journal of Alloys and Compounds*, *688*, 840-848. https://doi.org/10.1016/j.jphotochemrev.2017.12.002.

[104] Kumar, S., Sharma, V., Bhattacharyya, K., & Krishnan, V. (2016). Synergetic effect of MoS_2–RGO doping to enhance the photocatalytic performance of ZnO nanoparticles. *New Journal of Chemistry*, *40* (6), 5185-5197. https://doi.org/10.1039/C5NJ03595C.

[105] Tian, Q., Wu, W., Yang, S., Liu, J., Yao, W., Ren, F., & Jiang, C. (2017). Zinc oxide coating effect for the dye removal and photocatalytic mechanisms of flower-like MoS_2 nanoparticles. *Nanoscale research letters*, *12* (1), 1-10. https://doi.org/10.1186/s11671-017-2005-0.

[106] Liu, Y., Xie, S., Li, H., & Wang, X. (2014). A highly efficient sunlight driven ZnO nanosheet photocatalyst: synergetic effect of P-doping and MoS_2 atomic layer loading. *ChemCatChem*, *6* (9), 2522-2526. https://doi.org/10.1002/cctc.201402191.

[107] Kaur, M., Umar, A., Mehta, S. K., Singh, S., Kansal, S. K., Fouad, H., & Alothman, O. Y. (2018). Rapid solar-light driven superior photocatalytic degradation of methylene blue using MoS_2-ZnO heterostructure nanorods photocatalyst. *Materials*, *11* (11), 2254. https://doi.org/10.3390/ma11112254.

[108] Jo, W. K., Lee, J. Y., & Selvam, N. C. S. (2016). Synthesis of MoS_2 nanosheets loaded ZnO–g-C_3N_4 nanocomposites for enhanced photocatalytic applications. *Chemical Engineering Journal*, *289*, 306-318. https://doi.org/10.1016/j.cej.2015.12.080.

[109] Li, H., Wang, Y., Chen, G., Sang, Y., Jiang, H., He, J.,... & Liu, H. (2016). Few-layered MoS_2 nanosheets wrapped ultrafine TiO_2 nanobelts with enhanced photocatalytic property. *Nanoscale*, *8* (11), 6101-6109. https://doi.org/10.1039/C5NR08796A.

[110] Wang, D., Xu, Y., Sun, F., Zhang, Q., Wang, P., & Wang, X. (2016). Enhanced photocatalytic activity of TiO_2 under sunlight by MoS_2 nanodots modification. *Applied Surface Science*, *377*, 221-227. https://doi.org/10.1016/j.apsusc.2016.03.146.

[111] Wang, P., Shi, P., Hong, Y., Zhou, X., & Yao, W. (2015). Facile deposition of Ag_3PO_4 on graphene-like MoS_2 nanosheets for highly efficient photocatalysis. *Materials Research Bulletin*, *62*, 24-29. https://doi.org/10.1016/j.materresbull.2014.10.016.

[112] Chen, X., Zhang, J., Jiang, X., Wang, H., Kong, Z., Xi, J., & Ji, Z. (2018). Curved surface TiO_2 nanodrums coupled with MoS_2 as heterojunction photocatalysts with enhancing photocatalytic activity. *Materials Letters*, *229*, 277-280. https://doi.org/10.1016/j.matlet.2018.07.051.

[113] Zeng, L., Li, X., Fan, S., Yin, Z., Zhang, M., Mu, J.,... & Liu, S. (2019). Enhancing interfacial charge transfer on novel 3D/1D multidimensional MoS_2/TiO_2 heterojunction toward efficient photoelectrocatalytic removal of levofloxacin. *Electrochimica Acta*, *295*, 810-821. https://doi.org/10.1016/j.electacta.2018.10.153.

[114] Teng, W., Wang, Y., Huang, H., Li, X., & Tang, Y. (2017). Enhanced photoelectrochemical performance of MoS_2 nanobelts-loaded TiO_2 nanotube arrays by photo-assisted electrodeposition. *Applied Surface Science*, *425*, 507-517. https://doi.org/10.1016/j.apsusc.2017.06.297.

[115] Shao, N., Wang, J., Wang, D., & Corvini, P. (2017). Preparation of three-dimensional Ag_3PO_4/TiO_2@ MoS_2 for enhanced visible-light photocatalytic activity and anti-photocorrosion. *Applied Catalysis B: Environmental*, *203*, 964-978. https://doi.org/10.1016/j.apcatb.2016.11.008

[116] Tang, X., Wang, Z., Huang, W., Jing, Q., & Liu, N. (2018). Construction of N-doped TiO_2/MoS_2 heterojunction with synergistic effect for enhanced visible photodegradation activity. *Materials Research Bulletin*, *105*, 126-132. https://doi.org/10.1016/j.materresbull.2018.04.046.

[117] Liu, X., Xing, Z., Zhang, Y., Li, Z., Wu, X., Tan, S.,... & Zhou, W. (2017). Fabrication of 3D flower-like black N-TiO_2-x@ MoS_2 for unprecedented-high visible-light-driven photocatalytic performance. *Applied Catalysis B: Environmental*, *201*, 119-127. https://doi.org/10.1016/j.apcatb.2016.08.031.

[118] Zheng, L., Han, S., Liu, H., Yu, P., & Fang, X. (2016). Hierarchical MoS_2 nanosheet@TiO_2 nanotube array composites with enhanced photocatalytic and photocurrent performances. *Small*, *12* (11), 1527-1536. https://doi.org/10.1002/smll.201503441.

[119] Nimbalkar, D. B., Lo, H. H., Ramacharyulu, P. V. R. K., & Ke, S. C. (2016). Improved photocatalytic activity of RGO/MoS_2 nanosheets decorated on TiO_2 nanoparticles. *RSC advances*, *6* (38), 31661-31667. https://doi.org/10.1039/C6RA01591C.

[120] Li, X., Wen, J., Low, J., Fang, Y., & Yu, J. (2014). Design and fabrication of semiconductor photocatalyst for photocatalytic reduction of CO_2 to solar fuel. *Science China Materials*, *57* (1), 70-100. https://doi.org/10.1007/s40843-014-0003-1.

[121] Kumar, B., Asadi, M., Pisasale, D., Sinha-Ray, S., Rosen, B. A., Haasch, R. & Salehi-Khojin, A. (2013). Renewable and metal-free carbon nanofibre catalysts for carbon dioxide reduction. *Nature communications*, *4* (1), 1-8. https://doi.org/10.1038/ncomms3819.

[122] Chen, D., Zhang, H., Liu, Y., & Li, J. (2013). Graphene and its derivatives for the development of solar cells, photoelectrochemical, and photocatalytic applications. *Energy & Environmental Science*, *6* (5), 1362-1387. https://doi.org/10.1039/C3EE23586F.

[123] Deng, D., Novoselov, K. S., Fu, Q., Zheng, N., Tian, Z., & Bao, X. (2016). Catalysis with two-dimensional materials and their heterostructures. *Nature nanotechnology*, *11* (3), 218-230.

[124] Chu, S., & Majumdar, A. (2012). Opportunities and challenges for a sustainable energy future. *nature*, *488* (7411), 294-303.

[125] Herron, J. A., Kim, J., Upadhye, A. A., Huber, G. W., & Maravelias, C. T. (2015). A general framework for the assessment of solar fuel technologies. *Energy & Environmental Science*, *8* (1), 126-157.

[126] Li, L., Mu, X., Liu, W., Mi, Z. & Li, C. J. (2015). Simple and efficient system for combined solar energy harvesting and reversible hydrogen storage. *Journal of the American Chemical Society*, *137* (24), 7576-7579.

[127] Laurier, K. G., Vermoortele, F., Ameloot, R., De Vos, D. E., Hofkens, J., & Roeffaers, M. B. (2013). Iron (III)-based metal–organic frameworks as visible light photocatalysts. *Journal of the American Chemical Society*, *135* (39), 14488-14491. https://doi.org/10.1021/ja405086e.

[128] Khan, B., Raziq, F., Faheem, M. B., Farooq, M. U., Hussain, S., Ali, F.,... & Tian, H. (2020). Electronic and nanostructure engineering of bifunctional MoS_2 towards exceptional visible-light photocatalytic CO_2 reduction and pollutant degradation. *Journal of hazardous materials*, *381*, 120972. https://doi.org/10.1016/j.jhazmat.2019.120972.

[129] Hoffmann, M. R., Martin, S. T., Choi, W., & Bahnemann, D. W. (1995). Environmental applications of semiconductor photocatalysis. *Chemical reviews*, *95* (1), 69-96. https://doi.org/10.1021/cr00033a004.

[130] Wang, Z., & Mi, B. (2017). Environmental applications of 2D molybdenum disulfide (MoS_2) nanosheets. *Environmental science & technology*, *51* (15), 8229-8244. https://doi.org/10.1021/acs.est.7b01466.

[131] Xu, F., Zhu, B., Cheng, B., Yu, J., & Xu, J. (2018). 1D/2D TiO_2/MoS_2 hybrid nanostructures for enhanced photocatalytic CO_2 reduction. *Advanced Optical Materials*, *6* (23), 1800911. https://doi.org/10.1002/adom.201800911.

[132] Zheng, Y., Yin, X., Jiang, Y., Bai, J., Tang, Y., Shen, Y., & Zhang, M. (2019). Nano Ag-Decorated MoS_2 Nanosheets from 1T to 2H Phase Conversion for Photocatalytically Reducing CO_2 to Methanol. *Energy Technology*, *7* (11), 1900582. https://doi.org/10.1002/ente.201900582.

[133] Biswas, M. R. U. D., Ali, A., Cho, K. Y., & Oh, W. C. (2018). Novel synthesis of WSe_2-Graphene-TiO_2 ternary nanocomposite via ultrasonic technics for high photocatalytic reduction of CO_2 into CH_3OH. *Ultrasonics sonochemistry*, *42*, 738-746. https://doi.org/10.1016/j.ultsonch.2017.12.030.

[134] Fernandez-Ibanez, P., Byrne, J. A., López, M. I. P., Singh, A., McMichael, S., & Singhal, A. (2020). Photocatalytic inactivation of microorganisms in water. In *Nanostructured Photocatalysts* (pp. 229-248). Elsevier. https://doi.org/10.1016/B978-0-12-817836-2.00008-9.

[135] Yang, S., Shao, C., Zhou, X., Li, X., Tao, R., Li, X., & Liu, Y. (2020). $MoSe_2/TiO_2$ Nanofibers for Cycling Photocatalytic Removing Water Pollutants under UV–Vis–NIR Light. *ACS Applied Nano Materials*, *3* (3), 2278-2287. https://doi.org/10.1021/acsanm.9b02357.

[136] He, Z., Zhang, J., Li, X., Guan, S., Dai, M., & Wang, S. (2020). 1D/2D Heterostructured Photocatalysts: From Design and Unique Properties to Their Environmental Applications. *Small*, *16* (46), 2005051. https://doi.org/10.1002/smll.202005051.

[137] Xie, Z., Peng, Y. P., Yu, L., Xing, C., Qiu, M., Hu, J., & Zhang, H. (2020). Solar-Inspired Water Purification Based on Emerging 2D Materials: Status and Challenges. *Solar RRL*, *4* (3), 1900400. https://doi.org/10.1002/solr.201900400.

[138] Fu, S., Yuan, W., Liu, X., Yan, Y., Liu, H., Li, L. & Zhou, J. (2020). A novel 0D/2D WS_2/BiOBr heterostructure with rich oxygen vacancies for enhanced broad-spectrum photocatalytic performance. *Journal of colloid and interface science*, *569*, 150-163. https://doi.org/10.1016/j.jcis.2020.02.077.

[139] Vattikuti, S. P., Devarayapalli, K. C., Nagajyothi, P. C., & Shim, J. (2019). Binder-free WS_2/ZrO_2 hybrid as a photocatalyst for organic pollutant degradation under UV/simulated sunlight and tests for H_2 evolution. *Journal of Alloys and Compounds*, *809*, 151805. https://doi.org/10.1016/j.jallcom.2019.151805.

[140] Balasubramaniam, B., Singh, N., Kar, P., Tyagi, A., Prakash, J., & Gupta, R. K. (2019). Engineering of transition metal dichalcogenide-based 2D nanomaterials through doping for environmental applications. *Molecular Systems Design & Engineering*, *4* (4), 804-827. https://doi.org/10.1039/C8ME00116B.

[141] Li, X., & Peng, K. (2018). $MoSe_2$/montmorillonite composite nanosheets: hydrothermal synthesis, structural characteristics, and enhanced photocatalytic activity. *Minerals*, *8* (7), 268. https://doi.org/10.3390/min8070268.

[142] Wang, M., Peng, Z., Qian, J., Li, H., Zhao, Z., & Fu, X. (2018). Highly efficient solar-driven photocatalytic degradation on environmental pollutants over a novel C fibers@ $MoSe_2$ nanoplates core-shell composite. *Journal of hazardous materials*, *347*, 403-411. https://doi.org/10.1016/j.jhazmat.2018.01.013.

[143] Zhang, S., Chen, L., Shen, J., Li, Z., Wu, Z., Feng, W. & Zhang, S. (2019). TiO2@ MoSe2 line-to-face heterostructure: An advanced photocatalyst for highly efficient reduction of Cr (VI). *Ceramics International*, *45* (14), 18065-18072. https://doi.org/10.1016/j.ceramint.2019.06.027.

[144] Zhang, Y., Yang, X., Wang, Y., Zhang, P., Liu, D., Li, Y. & Gui, J. (2020). Insight into L-cysteine-assisted growth of Cu2S nanoparticles on exfoliated MoS2 nanosheets for effective photoreduction removal of Cr (VI). *Applied Surface Science*, 146191. https://doi.org/10.1016/j.apsusc.2020.146191.

[145] Liu, T., Li, Y., Du, Q., Sun, J., Jiao, Y., Yang, G. & Wu, D. (2012). Adsorption of methylene blue from aqueous solution by graphene. *Colloids and Surfaces B: Biointerfaces*, *90*, 197-203. https://doi.org/10.1016/j.colsurfb.2011.10.019.

[146] Wu, M. H., Li, L., Liu, N., Wang, D. J., Xue, Y. C., & Tang, L. (2018). Molybdenum disulfide (MoS_2) as a co-catalyst for photocatalytic degradation of organic contaminants: A review. *Process Safety and Environmental Protection*, *118*, 40-58. https://doi.org/10.1016/j.psep.2018.06.025.

[147] S. Adhikari, D.-H. Kim, Synthesis of Bi_2S_3/Bi_2WO_6 hierarchical microstructures for enhanced visible light driven photocatalytic degradation and photoelectrochemical sensing of ofloxacin, Chem. Eng. J., 2018, 354, 692-705 https://doi.org/10.1016/j.cej.2018.08.087.

[148] M. Chen, J. Yao, Y. Huang, H. Gong, W. Chu, Enhanced photocatalytic degradation of ciprofloxacin over $Bi_2O_3/(BiO)_2CO_3$ heterojunctions: Efficiency, kinetics, pathways, mechanisms and toxicity evaluation, Chem. Eng. J., 2018, 334, 453-461. https://doi.org/10.1016/j.cej.2017.10.064.

[149] M. Chen, W. Chu, Photocatalytic degradation and decomposition mechanism of fluoroquinolones norfloxacin over bismuth tungstate: Experiment and mathematic model, Appl. Catal. B: Environ., 2015, 168-169, 175-182. https://doi.org/10.1016/j.apcatb.2014.12.023.

[150] Li, L., Yan, Y., Liu, H., Du, J., Fu, S., Zhao, F.,... & Zhou, J. (2020). Hollow core/shell β-Bi_2O_3@WS_2 p–n heterojunction for efficient photocatalytic degradation of fluoroquinolones: a theoretical and experimental study. *Inorganic Chemistry Frontiers*, *7* (6), 1374-1385. https://doi.org/10.1039/C9QI01594A.

[151] Senthil, R. A., Osman, S., Pan, J., Sun, Y., Kumar, T. R., & Manikandan, A. (2019). A facile hydrothermal synthesis of visible-light responsive $BiFeWO_6/MoS_2$ composite as superior photocatalyst for degradation of organic pollutants. *Ceramics International*, *45* (15), 18683-18690. https://doi.org/10.1016/j.ceramint.2019.06.093.

[152] Ashraf, W., Bansal, S., Singh, V., Barman, S., & Khanuja, M. (2020). BiOCl/WS_2 hybrid nanosheet (2D/2D) heterojunctions for visible-light-driven photocatalytic degradation of organic/inorganic water pollutants. *RSC Advances*, *10* (42), 25073-25088. https://doi.org/10.1039/D0RA02916E.

[153] Fu, S., Liu, X., Yan, Y., Li, L., Liu, H., Zhao, F., & Zhou, J. (2019). Few-layer WS_2 modified BiOBr nanosheets with enhanced broad-spectrum photocatalytic activity towards various pollutants removal. *Science of The Total Environment*, *694*, 133756. https://doi.org/10.1016/j.scitotenv.2019.133756.